MOLECULAR AND CELLULAR BIOLOGY, Mar. 1997, p. 1714–1721 Vol. 17, No. 3
0270-7306/97/$04.00+0

Ultrabithorax and *Antennapedia* 5′ Untranslated Regions Promote Developmentally Regulated Internal Translation Initiation

XIN YE,[1] PETE FONG,[1] NARUSHI IIZUKA,[2] DONNA CHOATE,[1] AND DOUGLAS R. CAVENER[1]*

Department of Molecular Biology, Vanderbilt University, Nashville, Tennessee 37235,[1] and Department of Biochemistry, Biophysics, and Genetics, University of Colorado Health Science Center, Denver, Colorado 80262[2]

Received 2 November 1995/Returned for modification 18 December 1995/Accepted 13 December 1996

The 5′ untranslated regions (UTRs) of the *Drosophila Ubx* and *Antp* genes were tested for their ability to promote cap-independent translation initiation. The *Ubx* and the *Antp* 5′ UTR were inserted between the CAT and *lacZ* coding sequences in a dicistronic gene and tested for IRES activity in transgenic *Drosophila*. Northern analysis of the mRNAs showed the presence of the predicted full-length dicistronic mRNAs. High CAT activity was expressed from the first cistron from all of the dicistronic constructs introduced into the fly genome. The dicistronic transgenic strains bearing the *Ubx* and *Antp* IRES elements expressed significant levels of β-galactosidase (βGAL) from the second cistron whereas little or no βGAL was expressed in the controls lacking the IRESs. In situ analysis of βGAL expression in the transgenic strains indicates that expression of the second cistron is spatially and temporally regulated. Although the developmental patterns of expression directed by the Antp and Ubx IRESs overlap, they exhibit several differences indicating that these IRESs are not functionally equivalent.

The cap-independent internal initiation model was proposed initially to explain the mechanism of translation initiation of picornavirus mRNAs (2, 16–18, 25, 30, 35). The unique structural characteristics of picornoviral mRNAs including the absence of a cap structure at the 5′ end, the presence of extraordinarily long and structured 5′ untranslated regions (UTRs), and the presence of multiple upstream AUGs are incompatible with the cap-dependent scanning model purported to explain the translation of all cellular mRNAs. Upon infection of mammalian cells with poliovirus, the cap binding complex (eIF-4F) is inactivated due to the cleavage of the p220 (eIF-4Fγ) subunit of the cap-binding protein complex. Consequently, global translation of cellular mRNAs is inhibited while viral mRNAs are actively translated. These data suggested that the 40S preinitiation complex may bind a site remote from the 5′ terminus of the polioviral mRNA. Pelletier and Sonenberg (30) developed a dicistronic assay to detect the presence of internal ribosome entry sites (IRES, or ribosome landing pad). Expression of the downstream cistron was shown to be dependent upon the insertion of the poliovirus mRNA 5′ UTR in the intercistronic sequence (ICS) between the two cistrons. Moreover, blocking cap-dependent translation of the first cistron not only failed to block translation of the second cistron but actually elevated its level of translation.

Mapping experiments of poliovirus, encephalomyocarditis virus (EMCV), and human rhinovirus (HRV) demonstrated that a large segment (ca. 400 nucleotides [nt]) of the 5′ UTR is sufficient for enhancing translation in a cap-independent manner (5, 17, 30). It has been proposed that intrastrand RNA duplexes are essential for IRES activity (14, 17). Similar experiments have revealed that other picornavirus mRNAs are translated via internal initiation as well (2).

* Corresponding author. Mailing address: Department of Molecular Biology, Vanderbilt University, Nashville, TN 37235. Phone: (615) 322-3418. Fax: (615) 343-6707. E-mail: dcavener@ctrvax.vanderbilt.edu.

Although viral proteins may augment internal initiation either directly or indirectly, picornoviral proteins are translated efficiently without the presence of viral proteins. However, cellular factors are required for viral IRESs, but which factors are required varies among the picornaviruses. Rabbit reticulocyte lysate supports internal initiation of mRNAs bearing the EMCV IRES but not mRNAs with a HRV IRES. However, the addition of protein factors from HeLa cells can promote efficient translation of the latter (5). These results indicate that different protein factors may be required for different IRESs, suggesting the possibility of developmental regulation of internal initiation as a function of cell types.

A few cellular mRNAs have been found to contain IRESs. Sarnow and coworkers showed that the mRNA encoding GRP78/Bip (immunoglobulin binding protein) was translated at high levels during poliovirus infection when protein synthesis of most cellular proteins was depressed (24, 33). Subsequent experiments demonstrated that Bip mRNA is translated through a cap-independent/internal initiation mechanism. More recently the Drosophila *Antennapedia* (*Antp*) (28) and mouse fibroblast growth factor 2 (*Fgf2*) (39) mRNAs have been shown to contain IRES elements via the dicistronic assay system in transfected cells. Kim and coworkers (19) have shown the EMCV IRES is functional in transgenic mice. However, cellular mRNA 5′ UTR sequences, shown to provide IRES activity in transfected cells, have not been tested for IRES function or regulation in the context of whole animal development.

In principle, mRNAs which contain unusually long leader sequences with multiple upstream reading frames (URFs) are good candidates for initiating translation via a cap-independent internal ribosome binding mechanism. Among 380 *Drosophila* mRNAs analyzed, 39 have leader lengths exceeding 500 nt and contain multiple URFs (10). These include the developmentally important homeotic genes *Ultrabithorax* (*Ubx*) with a 968-nt 5′ UTR and two upstream AUGs and *Antp* with a 1,735-nt 5′ UTR (P2 mRNA) and 15 upstream AUGs (Fig. 1a).

We now show that the *Ubx* 5′ UTR contains an IRES which

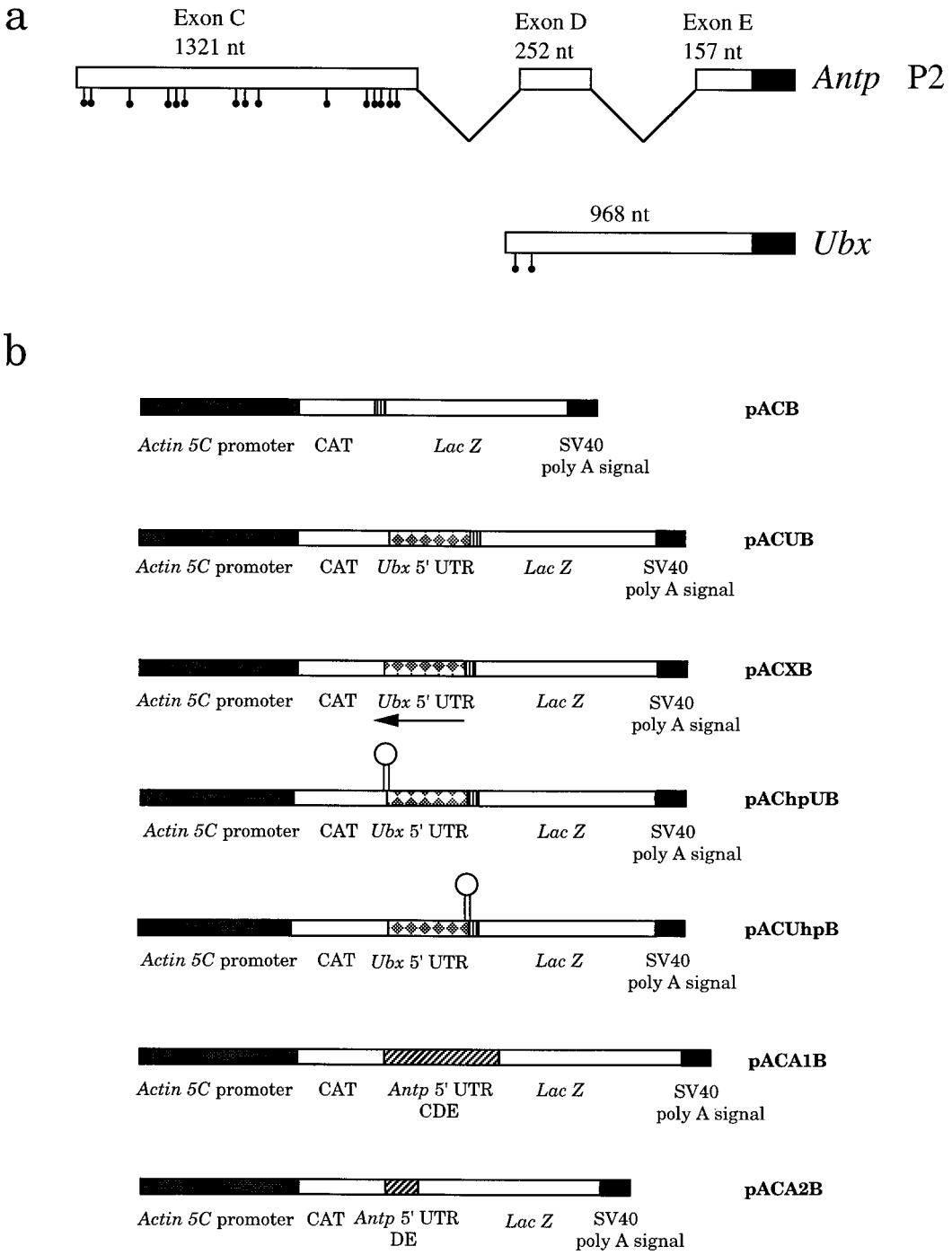

FIG. 1. Structure of the 5′ UTR region of the Drosophila *Antp* and *Ubx* mRNAs and the dicistronic genes. (a) The stippled rectangles represent the 5′ UTR sequence, and the solid rectangles represent 5′ end of the coding region. The lollipop symbols represent the position of upstream start codons (uAUGs). *Antp* P2, *Antp* transcript from the P2 promoter. (b) All dicistronic genes were constructed in a pCasPeR P-element vector and contain the *Actin 5C* distal promoter fused upstream of the bacterial *CAT* gene followed by a short intercistronic linker, the *lacZ* gene (containing a *Drosophila* translation initiation site), and the simian virus 40 polyadenylation (SV40 poly A) signal. The inserted 5′ UTR sequences of the *Ubx* and *Antp* genes are in their normal plus-strand orientation relative to the dicistronic mRNA except for pACXB. The hairpin symbols in pAChpUB and pACUhpB indicate the presence of a sequence designed to generate a stem-loop structure in the plus strand of the dicistronic mRNA.

can function in transfected cells and in transgenic *Drosophila*. In addition we show that the *Antp* 5′ UTR, previously demonstrated to act as an IRES in transfected cells (28), also acts as an IRES in transgenic *Drosophila*. For determining the IRES activity of *Ubx* and *Antp* 5′ UTRs, a constitutive promoter was used to drive the expression of dicistronic mRNAs so that the tissue-specific regulation of the IRES could be assessed throughout development. We show that the *Ubx* and *Antp* IRESs exhibit a high degree of developmental regulation.

MATERIALS AND METHODS

Plasmid construction. The *Actin 5C* distal promoter and the chloramphenicol acetyltransferase (CAT) gene coding region were obtained from a single plasmid, pAcCatLuc. pACB, the parental dicistronic construct for all the other plasmids, was made by subcloning a 3.2-kb *Bgl*II/*Bam*HI fragment from pAcCatLuc into a *Bam*HI site in pCaSpeRAUGβGAL (38). In pACB, two unique sites between the two cistrons, *Bam*HI and *Kpn*I, were utilized for inserting various sequences, including the 5′ UTR of *Ubx* and the hairpin-generating sequence (hpGem). Dicistronic pACUB was constructed in two steps. First, the 970-bp 5′ UTR of the *Ubx* gene was amplified from pT7Cat/Ubx/Luc (gift from P. Sarnow's lab) by PCR, incorporating *Bam*HI and *Bgl*II sites at the 5′ and 3′ ends of the fragment, respectively. In the second step, a restriction-digested PCR fragment was subcloned into the *Bam*HI site in pACB, resulting in pACUB (*Ubx* 5′ UTR in the plus orientation) and pACXB (*Ubx* 5′ UTR in the reverse orientation). The hairpin-generating sequence hpGem (24, 28), predicted to have a duplex strength (ΔG) of −60 kcal/mol, was inserted in the *Bam*HI site between CAT and *Ubx* 5′ UTR in pACUB, generating pAChpUB, and also inserted in the *Kpn*I site between the *Ubx* 5′ UTR and *lacZ* in pACUB, generating pACUhpB.

The plasmids containing *Antp* 5′ UTR sequences, pACA1B and pACA2B, were constructed as follows. A *Bam*HI-*Xba*I fragment containing the simian virus 40 poly(A) addition sequence was inserted downstream of an *Actin 5C* promoter-CAT gene present in the P-element *white* vector yielding p6. To generate pACA1B, a 4.8-kb *Xba*I fragment from pTF1, containing the *Antp* P2 5′ UTR present in exons C, D, and E fused to a nucleus-targeted *lacZ* gene, was inserted into the *Xba*I site of p6 downstream of the CAT gene. To generate pACA2B, a 2.6-kb *Xba*I fragment from pTF2, containing the *Antp* P2 5′ UTR present in exons D and E fused to a nucleus-targeted *lacZ* gene, was inserted into the *Xba*I site of p6 downstream of the CAT gene.

Cell culture and transfection experiments. *D. melanogaster* Schneider SL2 cells were grown at 25°C in Schneider's Drosophila medium (GIBCO BRL, Inc.) containing 10% heat inactivated fetal bovine serum (Irvine Sci. Co.). At 36 h before transfection, cells were plated at a density of 5×10^6 cells per 60-mm plate. Cells were transfected by using Lipofectin (GIBCO BRL, Inc.). Before transfection the old medium was replaced with new Schneider's medium without bovine serum or antibiotics. Five micrograms of supercoiled DNA was mixed with 20 μg of Lipofectin in a total volume of 100 μl and incubated at room temperature for 15 min. After incubation, the DNA-Lipofectin complex was added to the cells dropwise. After 5 h of incubation at 25°C, 10% fetal bovine serum was added. Cells were harvested 48 h after transfection.

P-element transformation. *D. melanogaster* embryos were injected with appropriate plasmid DNAs by the general procedure of Rubin and Spradling (32). All these transformant plasmids carry the *Drosophila white* gene as a selectable marker. The host strain ES3 is a *w* mutant which has constitutive P-element transposase activity (31). Adult survivors (G0) were crossed singly to ES3 flies, and their progeny (G1) were screened for red eyes. Genetic crosses were done to determine which chromosomes contained the transduced genes and to replace the endogenous β-galactosidase (βGAL) wild-type gene with the βGAL null mutant (20). All of the transgenic flies were named after the dicistronic transgenes they carried.

Northern analysis. Small-scale RNA preparations were used for developmental Northern analysis. Total RNA was isolated from flies or dissected tissues as described previously (9). For some samples, poly(A)$^+$ RNA was prepared from total RNA by using oligo(dT) affinity chromatography.

Total RNA or poly(A)$^+$ RNA samples were fractionated on a 1.2% agarose gel containing 6% formaldehyde. After electrophoresis, the RNA was transferred to a nylon membrane (Hybond-N; Amersham) and cross-linked to the membrane by UV irradiation (305-nm transilluminator). Various cRNA probes were radiolabeled by in vitro transcription using [^{32}P]UTP. The Northern blots were hybridized to the cRNA probes in the presence of 50% formamide at 59°C, washed, and exposed to autoradiography film.

Histochemical analysis. In situ βGAL staining of dissected *Drosophila* tissues was done by using a modified histochemical staining method developed by Glaser and coworkers (13). Flies (larvae, pupae, or adults) were dissected in 10 mM sodium phosphate (pH 7.0)–150 mM NaCl–1 mM $MgCl_2$ containing 1% glutaraldehyde at room temperature. Dissected tissues were rinsed in 10 mM sodium phosphate (pH 7.0)–150 mM NaCl–1 mM $MgCl_2$–3.3 mM $K_3[Fe(III)CN_6]$–3.3 mM $K_4[Fe(II)CN_6]$ and then in 10 mM sodium phosphate (pH 7.0)–150 mM NaCl–1 mM $MgCl_2$–3 mM $K_3[Fe(III)CN_6]$–3 mM $K_4[Fe(II)CN_6]$. Tissues were stained in 0.2% X-Gal (5-bromo-4-chloro-3-indolyl-β-D-galactopyranoside) at room temperature in the dark for 15 min to overnight as necessary. Embryos were staged and stained en masse with X-Gal (1, 3). Embryos were dechorionated in 50% commercial Clorox bleach and fixed with fixative {0.08 M PIPES [piperazine-*N*,*N*′-bis(2-ethanesulfonic acid)] (pH 6.9), 1.6 mM EGTA, 0.8 mM $MgSO_4$, 7.4% formaldehyde} and *n*-heptane. Fixed embryos were then removed from the organic/aqueous interface and placed in the wells of a microtiter plate. After residual heptane/fixative was removed, Triton/PBS (0.3% Triton X-100 in phosphate-buffered saline [PBS]) was added to the embryos. When the embryos had sunk below the surface, the Triton/PBS buffer was replaced with Fe/Na staining medium {10 mM sodium phosphate, 150 mM NaCl, 1 mM $MgCl_2$, 6.1 mM $K_3[Fe(III)CN_6]$, 6.1 mM $K_4[Fe(II)CN_6]$, 0.2% X-Gal, 0.3% Triton X-100}. Stained samples were rinsed with PBS (10 mM sodium phosphate, pH 7.0/150 mM NaCl; 1 mM $MgCl_2$). Specimens were photographed on Kodak Gold 200 print films with an Olympus OM-1 camera under either a Zeiss Universal or a Nikon SMZ-10 microscope.

βGAL and CAT assays. A quantitative βGAL enzymatic assay was performed as described previously (34). Flies were homogenized in 100 μl of assay buffer (50 mM potassium phosphate [pH 7.5], 1 mM $MgCl_2$). An aliquot of the supernatant was transferred to a cuvette containing 2 ml of chlorophenol red β-D-galactopyranoside (CPRG) solution (1 mM CPRG in assay buffer), and incubated at 37°C. Optical density readings at 574 nm were taken at intervals of 30 s over a period of 30 min in a thermostat spectrophotometer. The resulting slope (change in A_{574}/min) was used to estimate βGAL activity. One unit of βGAL enzyme activity is equal to 1.0 μmol of CPRG hydrolyzed per min per fly.

CAT assays were done after the methods of Neumann and coworkers (27) with minor modifications: flies or dissected tissues were homogenized in 100 mM Tris-HCl (pH 7.5). The homogenate was incubated at 65°C for 5 min to precipitate most proteins and inactivate any inhibitor(s) of CAT. After centrifugation at 14,000 rpm at 4°C, an aliquot of the supernatant was mixed in a scintillation vial with 100 mM Tris-HCl (pH 7.5) (up to a total volume of 50 μl), 200 μl of premix (1.25 mM chloramphenicol in 100 mM Tris-HCl [pH 7.5]), and 0.1 mCi of [^{14}C]-butyryl coenzyme A (CoA) (DuPont, NEN Research Products). The reaction mix was overlaid with 5 ml of Econofluor-2 (DuPont, NEN Research Products) and incubated at room temperature in a scintillation counter. Conversion of chloramphenicol to butyryl chloramphenicol was measured as ^{14}C counts per minute by scintillation counting at intervals of 10 to 20 min over a period of 2 h. The resulting changes in counts per minute over the assay period were used to determine the units of CAT activity in each sample based on an experimental standard curve. One unit of CAT enzyme activity is equal to 1.0 nanomole of chloramphenicol and acetyl-CoA converted to chloramphenicol 3-acetate and CoA per minute per fly.

In situ localization of transgenic mRNA. A hybridization probe for the dicistronic mRNAs was generated by labeling the *Escherichia coli lacZ* gene with digoxigenin (DIG)-dUTP via random-primed labeling with the Genius Nonradioactive Nucleic Acid and Detection System (Boehringer Mannheim, Inc.). Embryos, 0 to 24 h old, were dechorionated, fixed with paraformaldehyde, treated with proteinase K, and then hybridized overnight at 45°C with the DIG probe by the procedures of Tautz and Pfeifle (37). The DIG-*lacZ* mRNA hybrids were detected by alkaline phosphatase-conjugated anti-DIG antibody followed by treatment with nitroblue tetrazolium (NBT) and 5-bromo-4-chloro-3-indolylphosphate toluidinium (BCIP) for 3 to 120 min.

RESULTS

***Ubx* 5′ UTR functions as an IRES in transfected *Drosophila* cells.** A dicistronic gene (pACB) was constructed by using the bacterial CAT gene and the *lacZ* gene encoding βGAL under transcriptional control of the *Drosophila Actin 5C* distal promoter (Fig. 1b). The 5′ UTR of *Ubx* 5′ UTR was inserted between the two cistrons of this plasmid, yielding pACUB, to test for its ability to act as an IRES. To provide a nonspecific control, the *Ubx* 5′ UTR was reversed relative to its normal orientation and inserted between the two cistrons (pACXB). To control for the potential cap-dependent termination-reinitiation of the second cistron, a potential hairpin-generating sequence was inserted between the first cistron and the *Ubx* 5′ UTR (pAChpUB). The efficacy of this hairpin structure to block ribosome scanning was examined by constructing a plasmid with the hairpin-generating sequence between the *Ubx* 5′ UTR and the second cistron (pACUhpB). Thus, the hairpin structure in pAChpUB should not interfere with internal initiation promoted by the *Ubx* 5′ UTR whereas the hairpin structure placed downstream of the *Ubx* 5′ UTR should block translation of the second cistron in pACUhpB.

The five dicistronic plasmids described were transfected into *Drosophila* SL2 cells and assayed for CAT and βGAL activity 48 h after transfection. In two independent experiments, moderate to high levels of CAT activity were seen for all five plasmids tested (Table 1). In contrast, the expression of the second cistron, βGAL, varied over a range of 327-fold. CAT activity should be directly proportional to the transfection efficiency and level of dicistronic mRNA, and therefore we have normalized βGAL activity to CAT activity to estimate the IRES activity of the *Ubx* 5′UTR. In addition these ratios were normalized to the CAT/βGAL ratio for the pACB transfections since pACB lacks the *Ubx* 5′UTR. The average IRES

TABLE 1. Expression of βGAL and CAT activities in dicistronic genes containing *Ubx* 5′ UTR in transfected SL2 cells

Plasmid	Mean activity (SD)	
	βGAL	CAT
pACB	0.03 (0.01)	0.35 (0.01)
pACUB	2.07 (0.35)	1.19 (0.23)
pACXB	0.31 (0.11)	0.98 (0.27)
pAChpUB	9.80 (2.38)	0.75 (0.37)
pACUhpB	0.09 (0.04)	0.93 (0.09)

activity of pACUB was 21, whereas its minus orientation counterpart was 3.2 (Fig. 2). Transfection of pAChpUB consistently yielded the highest IRES activity (164) whereas its 3′ positioned hairpin construct counterpart (pACUhpB) yielded the lowest IRES activity (1.2) as expected. Thus the hairpin-generating sequence greatly augments the IRES activity of *Ubx* in a 5′ position but completely blocks it when positioned between the *Ubx* 5′ UTR and *lacZ*.

***Ubx* and *Antp* 5′ UTRs function as IRESs in transgenic *Drosophila*.** *Drosophila* transgenic strains were obtained for the dicistronic plasmids pACB, pACUB, pACXB, pACA1B, and pACA2B via P-element-mediated transformation. pACB lacks any additional sequences between the CAT and *lacZ* genes and serves as the basic negative control for plasmids that contain either the *Ubx* 5′ UTR (pACUB and pACXB) or the *Antp* 5′ UTR (pACA1B and pACA2B). (See above for further description of the *Ubx* constructs.) pACA1B contains the entire 5′ UTR of *Antp* P2 mRNA (exons C, D, and E) whereas pACA2B contains only 5′ UTR sequences present in exons D and E (Fig. 1). The transgenic strains were made homozygous for the transgenes and placed in a βGal^{-} mutant background to avoid background expression of βGAL from the *Drosophila* endogenous βGal gene. These strains are referred to by their plasmid names (minus the p prefix). At least two transgenic strains for each construct were analyzed, and the patterns of βGAL expression discussed below were consistent among these strains unless otherwise stated.

To quantitatively estimate the IRES activity in the transgenic strains, CAT and βGAL enzyme assays were performed on whole-fly homogenates. The ratios of βGAL activity to CAT activity (βGAL/CAT) were used to estimate relative

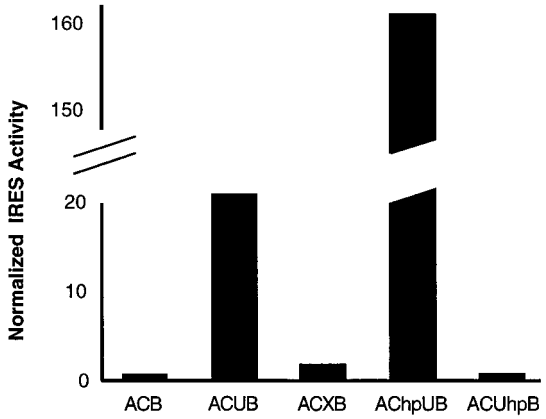

FIG. 2. IRES activity of the *Ubx* 5′ UTR in transfected cells. IRES activity was calculated as the ratio of βGAL activity to CAT activity (Table 1) normalized to the βGAL/CAT ratio of ACB. The values shown are the averages of two independent transfection experiments.

TABLE 2. Quantitative expression of βGAL and CAT activities in transgenic *Drosophila*

Strain	Activity	
	βGAL	CAT
Third-instar larva		
ACB	0.32	0.1020
ACUB	2.72	0.2908
ACA1B	128.59	0.2882
ACA2B	10.18	0.3918
Pupa		
ACB	1.01	0.2056
ACUB	7.46	0.3601
Pharate adult		
ACB	0.27	0.2086
ACUB	2.24	0.6453
Adult		
ACB	0.10	0.0794
ACUB	1.00	0.1811

IRES activity. Although the CAT enzyme activities varied over fourfold among lines and developmental stages, βGAL activities ranged over 3 orders of magnitude. Thus the differences in the βGAL/CAT ratios are mostly contributed by large differences in βGAL activities. Four developmental stages for the *Ubx* constructs and the ACB negative control were assayed: wandering third-instar larvae, early pupae, pharate adults (late pupae), and adults (Table 2). The IRES activity of the ACUB transgenic strains were 2.7- to 4.4-fold higher than the ACB lines (Fig. 3). For the *Antp* constructs ACA1B and ACA2B, third-instar larvae were quantitatively assayed for IRES activity. The ACA1B transgene shows the highest IRES activity: 142-fold higher than ACB and 17-fold higher than ACA2B

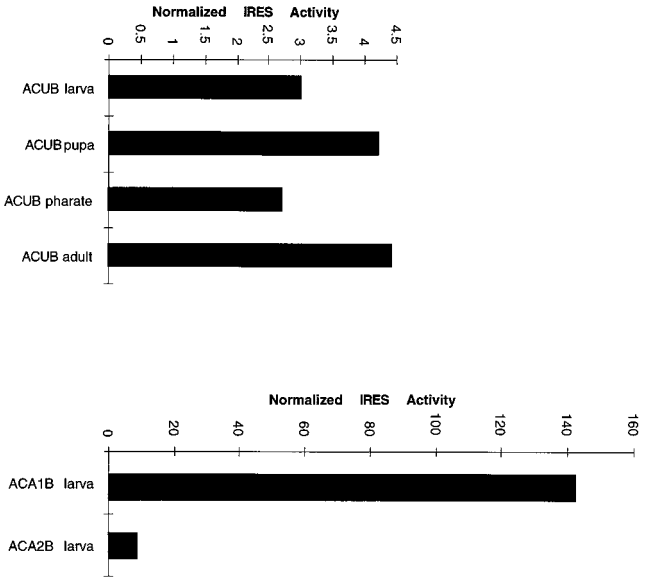

FIG. 3. IRES activity of the *Ubx* and *Antp* 5′UTRs in transgenic Drosophila strains. IRES activity was calculated as the ratio of βGAL activity to CAT activity (Table 2) normalized to the βGAL/CAT ratio of ACB. Each value represents the mean of two independent transgenic strains. Larva, third instar larvae; pupa, stage 3 to 5 pupae; pharate, stage 12 to 15 pharate adults; adult, 3- to 7-day-old adults.

FIG. 4. Tissue-specific expression of dicistronic mRNAs. DIG-labeled *E. coli lacZ* DNA was hybridized to 0- to 24-h-old embryos. Subsequently the DIG-labeled hybrids were detected with an anti-DIG-alkaline phosphatase conjugate and visualized with NBT and BCIP. (a) Negative control strain, Δ2-3, lacking heterologous *lacZ* exhibits no signal over a 2-h period. (b) Positive control strain *Gld/lacZ 182.9* exhibits signal in the antennomaxillary complex (upper right lateral structures) and labial region (upper right central structures) only. Signal was detected after 45 min. (c) ACUB exhibits expression in all tissues after 3 to 5 min. (d) ACA1 exhibits expression in all tissues after 3 to 5 min. All stages of embryos (preblastoderm, blastoderm, and all later stages) were observed to stain heavily in the ACUB and ACA1 embryos. Two independent experiments were performed, yielding the same results.

(Fig. 3). OH and coworkers (28) previously showed in transfected SL2 cells that the IRES activity of the full *Antp* P2 5′ UTR (corresponding to ACA1B) was only about threefold higher than the truncated *Antp* P2 5′ UTR missing exon C (corresponding to ACA2B).

The *Actin 5C* promoter used in these experiments is known to normally drive high constitutive levels of expression throughout development (6). However to rule out the possibility that the dicistronic reporter genes and the *Antp* and *Ubx* 5′ UTRs did not abrogate or modify the activation of this promoter in our constructs, we examined the expression of the ACA1 and ACUB mRNAs in situ by using a probe for *lacZ*. As expected, a very high level of expression of these mRNAs were detected in all tissues throughout embryogenesis (Fig. 4c and d). In contrast, no signal was detected in control embryos lacking *E. coli lacZ* (Fig. 4a) and a highly tissue-specific pattern of expression was observed in a transgenic strain bearing a *Gld/lacZ* transgene (Fig. 4b). In the latter case, the mRNA and βGAL histochemical patterns of expression were precisely coincident, unlike ACA1 and ACUB, in which only the βGAL enzyme was highly tissue specific (see below). These controls substantiate the posttranscriptional regulation of βGAL in ACA1 and ACUB. Correlated with the abundance of dicistronic mRNAs was a high level of CAT enzyme activity detected throughout embryogenesis (data not shown).

To assess the tissue-specific activity of the *Ubx* and *Antp* IRESs, βGAL expression patterns were determined in situ. βGAL was first detected in stage 16 to 17 embryos in the *Ubx* ACUB transgenic strains whereas βGAL was not detected at any embryonic stage in the ACB, ACXB, ACA1B, and ACA2B transgenic strains (Table 3). In the ACUB transformants, βGAL activity was consistently detected in the proventriculus.

TABLE 3. Tissue-specific expression of β-GAL in dicistronic transgenic flies

Stage/tissue[a]	Expression[b]					
	ACUB	ACXB	ACA1B	ACA2B	ACB	K1CV9
Embryo						
Hypoderm	+/−	−	−	−	−	−
Proventriculus	++	−	−	−	−	−
Midgut	+	−	−	−	−	−
Third-instar larva						
Anterior spiracular gland	−	+/−	+	+	−	−
Salivary glands	++	−	−		+/−	−
Proventriculus	+	−	++	+	−	−
Foregut imaginal ring	+++	−	++	++	+/−	−
Intestinal tract	++	−	+++	++	−	−
Hypoderm	+/−	−	−	−	−	−
Imaginal discs	−	−	−	−	−	−
Pharynx	−	−	++	+	−	−
Fat body cells	−	−	+++	++	+/−	−
Trachea/intestine junctions	−	−	+++	−	−	−
Pharate adult						
Antenna	+/−	−	−	−	−	−
Maxillary palps	−	−	++	+	−	
Labial palps	+/−	−	++	+	−	−
Proboscis	−	−	++	+	−	−
Wings and halteres	++	−	++	+	+/−	−
Legs	−	−	−	−	−	−
Head hypoderm	+/−	−	++	+	−	−
Thoracic hypoderm	++	+/−	+++	+	+/−	−
Abdominal hypoderm	−	+/−	−	−	−	−
Fat body	−	−	+++	+	−	−
Intestinal tract	na	na	+++	+	−	−
Adult						
Fat body	−	−	+	−	−	−
Intestinal tract	−	+/−	+++	++	−	−
Thoracic muscles	+++	−	−	−	+/−	−
Thoracic/leg joint	−	−	+	+	−	−
Thoracic/wing joint	−	−	−	−	−	−
Rectal papillae	+	−	+	−	+/−	−
Testis coils (M)	++	−	+	+	+/−	−
Ejaculatory bulb (M)	−	+/−	−	−	−	−
Seminal receptable (F)	−	−	+	+	−	−
Spermatheca (F)	−	+/−	−	−	−	−
Uterus (F)	−	+/−	+	+	−	−

[a] F, female; M, male.
[b] +++, high; ++, moderate; +, low; +/−, variable; −, not expressed; na, not assayed.

The proventriculus forms in late embryogenesis (stage 16 to 17) when the cells of the anterior midgut overgrow the posterior end of the foregut, producing the characteristic funnel-like cardiac structure (7). In addition, βGAL was frequently detected in the midgut of these embryos.

Third-instar larvae from the ACUB transgenic strains showed high expression of βGAL in the distal two thirds of the salivary glands and the foregut imaginal ring encircling the proventriculus. In the hypoderm, βGAL activity was detected in a dispersed area. The major stained tissues were the intestinal tract and the hypoderm (Table 3). Endogenous *Ubx* is expressed predominantly in the third thoracic imaginal discs (third leg discs and haltere discs). However, βGAL was not detected in these discs in the ACUB transformants. Third-instar larvae from the *Antp* constructs ACA1B and ACA2B exhibited high levels of βGAL in the intestinal tract and foregut imaginal ring and a lower level in the anterior spiracles (Table 3). The ACA1B strains also showed high levels of expression in the fat body cells and tracheal-intestinal junctions. βGAL was not expressed in thoracic imaginal discs, brain, or ventral nerve cord, where ANTP protein is normally expressed. However, ANTP is expressed in the larval gut, where βGAL is also expressed in the ACA1B and ACA2B transgenic strains.

At the pharate adult stage (late pupal), the ACUB animals expressed a high level of βGAL in the thorax, wings and halteres, and abdominal hypoderm (Table 3). For the *Antp* constructs ACA1B and ACA2B, moderate to low levels of βGAL were observed in the labium, maxillary palps, proboscis, fat body, intestinal tract, and head and thoracic hypoderm (Table 3). Some of these tissues also express ANTP.

Mature adults (>5 days old) were examined for all of the transformant strains. ACUB adult flies exhibited high βGAL expression in the thoracic muscles (Table 3), the intestinal tract, testes, and rectal papillae. Adult males of the *Antp* ACA1B and ACA2B strains showed high levels of expression in the intestinal tract and lower levels in the thorax, legs, and testes; females showed low levels of expression in the seminal receptacle, anterior uterus, and vaginal plate. In all developmental stages the parental nontransformant K1CV9 βGal$^-$ strain showed no appreciable βGAL activity in any of the tissues described above that express βGAL in the transgenic strains.

Dicistronic transgenes produce abundant full-length dicistronic mRNAs. A key assumption of the dicistronic assay for IRES activity is that full-length dicistronic mRNA will be faithfully produced. Northern blot analysis was used to investigate the integrity of the mRNAs isolated from the transgenic flies at various developmental stages. For the *Ubx* 5′ UTR transgenic strains and negative controls, CAT and LacZ probes were used independently to ensure that both coding sequences were present in the presumed dicistronic mRNAs. As shown in Fig. 5A (lanes 1 to 7), the predicted mRNAs for the ACB (5.4 kb), ACUB (6.4 kb), and ACXB (6.4 kb) were observed by using the CAT cRNA probe. These are the appropriate sizes for the full-length dicistronic mRNAs. The βGAL cRNA probe detected the same mRNA species (Fig. 5A, lanes 10 to 16) as well as a smaller RNA (4.2 kb) in most of the transformant lines. The presence and size of these smaller transcripts did not depend on the presence of the 5′ UTR of *Ubx* in these dicistronic transgenes, suggesting that they started downstream of the ICS. Similar Northern hybridization was also performed on the total RNAs isolated from pupae and embryos. Similar results were observed: only one intact dicistronic transcript was hybridized to the CAT probe while two RNAs were detected by the LacZ probe (data not shown). Importantly, the presence of the unexpected 4.2-kb RNA was not correlated with βGAL enzyme expression since the ACB transgenic flies exhibit the 4.2-kb RNA but expressed very little if any βGAL enzyme activity (Table 3).

Northern blot analysis of the *Antp* 5′ UTR transgenic strains exhibited the predicted full-length mRNAs in embryos and third-instar larvae (Fig. 5B and C). The ACA1B transgenic strains show a 6.7-kb mRNA whereas the ACA2B transgenic strains, which contain 1,321 nt less 5′ UTR, exhibit a 5.4-kb mRNA as detected by a *lacZ* probe. Embryos express the ACA1B and ACA2B transgene mRNA (Fig. 5C) and high levels of CAT enzyme activity (data not shown) but do not express βGAL enzyme activity (Table 3). In contrast, third-instar larvae express high levels of the transgene mRNAs (Fig. 5B) and CAT and βGAL enzyme activities (Tables 2 and 3). CAT enzyme activity is highly correlated with the presence of the dicistronic mRNA, independent of the transgenic strains, whereas βGAL enzyme activity is dependent upon the pres-

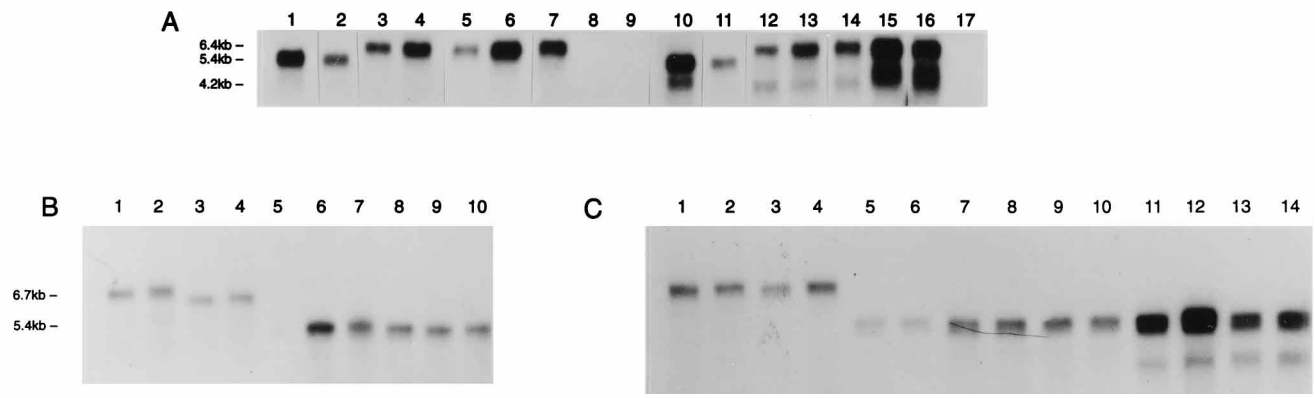

FIG. 5. Northern analysis of the dicistronic transgenic strains. CAT or *lacZ* radiolabeled cRNA probes were hybridized to Northern blots of total RNA. (A) Adult RNA; lanes 1 to 9 hybridized with CAT probe; lanes 10 to 17 hybridized with LacZ probe. Lanes: 1 and 10, ACB-25; 2 and 11, ACB-5; 3 and 12, ACUB-6R; 4 and 13, ACUB-2; 5 and 14, ACXB 32; 6 and 15, AChpUB29; 7 and 16, AChpUB 8.2; 8, 9, and 17, K1CV9. Note: upon longer exposure a 4.2-kb RNA is also detected in lane 11. (B) Third-instar larva RNA hybridized with LacZ probe. Lanes: 1 and 2, ACA1B-1; 3 and 4, ACA1B-7; 5, blank; 6, ACA2B-4; 7 and 8, ACA2B-12; 9 and 10, ACA2B-16. (C) Embryonic RNA hybridized with LacZ probe. Lanes: 1 and 2, ACA1B-1; 3 and 4, ACA1B-7; 5 and 6, ACA2B-4; 7 and 8, ACA2B-12; 9 and 10, ACA2B-16; 11 and 12, ACB-25; 13 and 14, ACB-G1.

ence of the *Antp* 5′ UTR and exhibits complex tissue-specific patterns of expression.

DISCUSSION

The 5′ UTRs of three cellular mRNAs (Drosophila *Antp* and mammalian *bip* and *Fgf2*) were previously shown to promote cap-independent translation by a dicistronic assay system in transfected cells. A major outstanding question regarding cellular IRESs is whether they promote constitutive translation initiation (similar to cap-dependent initiation) or whether their activities are developmentally regulated. Comparative studies of the viral HRV and EMCV IRESs predicted that IRES activity may be developmentally regulated, because they differed in their requirement for host cell factors (5). However, this assumption has not been tested. To determine whether cellular IRESs are constitutive or regulated, it is desirable to express the test dicistronic mRNA constitutively in a whole-animal system so that the regulation of IRES activity can be assessed in any tissue or stage. Consequently, we constructed a dicistronic gene under the control of a strong constitutive promoter. From the resultant transgenic strains we found that the *Ubx* and *Antp* IRES activities are highly developmentally regulated. Temporally, *Ubx* IRES activity is seen in all the major life cycle stages (embryos, larvae, pupae, and adults). *Ubx* IRES activity is not seen until late embryogenesis, where it is pronounced in the developing proventriculus. In contrast, no *Antp* IRES activity is seen in the embryonic proventriculus or in any other embryonic tissue despite high levels of dicistronic mRNA. Moreover, the negative control transgenes (ACB and ACXB) also do not show expression of βGAL in the embryonic proventriculus. Thus, the high βGAL expression of ACUB in this organ during embryonic development uniquely requires the 5′ UTR of *Ubx*. Curiously, during larval development both the *Ubx* and *Antp* IRESs promote high βGAL expression in the foregut imaginal ring, which constitutes part of the proventriculus.

An important design feature of our dicistronic assay for IRES function of *Ubx* was the inclusion of a strong hairpin-generating sequence, hpGEM ($\Delta G = -60$ kcal/mol), to block the transit of the scanning 40S preinitiation complex. The hpGEM sequences was successfully used previously for blocking translation in COS cells (24, 28). Insertion of the hairpin sequence between the first cistron and the *Ubx* 5′ UTR should block any 40S complex which may have terminated translation of the first cistron and resumed scanning or which may have bound internally in the CAT sequence. The ability of this hairpin sequence to block scanning in transfected cells was tested critically by inserting it between the *Ubx* 5′ UTR and the second cistron. As expected, the hairpin completely blocked translation of the second cistron whereas insertion upstream of the *Ubx* 5′UTR actually enhanced translation of the second cistron.

The developmental expression controlled by the *Ubx* and *Antp* IRESs in transgenic strains is partially correlated with the major tissues expressing the UBX and ANTP proteins, respectively. The *Ubx* IRES is active in the embryonic hypoderm midgut, and proventriculus, tissues that also express the UBX protein (40). Recently, *Drosophila* La (homolog of mammalian La autoantigen) mutants have been shown to have reduced or absent levels of UBX protein in the embryonic midgut (38a). Since mammalian La autoantigen has been strongly implicated as a major effector of IRES function (36), this is an intriguing finding. However, the embryonic central nervous system and larval imaginal tissues, two major sites of UBX and ANTP expression (8, 40), did not exhibit *Antp* and *Ubx* IRES activity in our assays despite high levels of dicistronic mRNAs in these tissues. Three explanations for this lack of concordance may be considered. (i) *Ubx* may use cap-dependent or cap-independent mechanisms for translation initiation depending upon the specific tissue and/or stage. Most likely the *Ubx* mRNA contains a cap structure at its 5′ terminus and therefore would have the possibility of being translated in a cap-dependent mechanism. It is much less likely that *Antp* uses a cap-dependent mechanism for translation because its 5′ UTR contains 15 upstream ORFs. (ii) The methods used to assess the developmental specificity of IRES activity may not be sensitive enough to detect transient expression. If, for example, IRES activity is restricted to a brief period of time during the cell cycle, then the level of the expression of the *lacZ* reporter may be too low to detect. (iii) Other segments of the *Ubx* and *Antp* mRNAs may be essential for proper IRES developmental regulation. Since no other cellular IRES has been investigated in the context of development, it is unknown whether the IRESs identified so far are sufficient for proper regulation. A large number of recently characterized developmentally regulated mRNAs contain 3′ UTR sequences which are thought to interact with the 5′ cap and/or 5′ UTR to mediate control of translation initiation.

mRNAs with unusually long 5′ UTRs in *Drosophila* and vertebrates encode, almost exclusively, regulatory proteins (10, 22). These mRNAs typically contain multiple upstream AUGs. Kozak (21, 22) has argued that these types of mRNAs are all translated by a cap-dependent mechanism and has proposed that the upstream AUGs are ignored by the scanning preinitiation complex (leaky scanning) because they contain a poor sequence context. A thorough analysis of sequence context data by Cavener and Ray (11) and mutagenesis of translation start site context in *Drosophila* (12) does not support the conclusion that upstream AUGs would typically be ignored by the mechanism of leaky scanning. Consequently, it seems unlikely that mRNAs such as *Antennapedia*, which contain 15 upstream AUGs, could be translated via cap-dependent mechanism since traversing the long leader would require numerous rounds of termination-reinitiation, a process known to be inefficient (26). The data presented herein support the hypothesis that *Antp* and *Ubx* are translated via a cap-independent mechanism.

Cap-independent IRES-mediated initiation may enable the selective translation of specific mRNA species under varying physiological conditions that are disassociated from cap-dependent initiation, a process which is highly regulated (4, 23, 29). We speculate that developmental regulatory proteins, which constitute a small fraction of bulk protein synthesis, may utilize IRES-mediated translation as a means of specifying changes in cell differentiation and proliferation during mitosis, when global protein synthesis is temporarily repressed.

ACKNOWLEDGMENTS

We thank Ed Organ for microinjecting the transgenes, Peter Sarnow for technical advice and the gift of DNA clones used in the construction of the dicistronic genes, and DeAnne Olsen and Sara Perlaky for editing the manuscript.

This work was supported by NSF grant MCB-9304983.

REFERENCES

1. **Bellen, H. J., et al.** 1989. P-element-mediated enhancer detection: a versatile method to study development in *Drosophila*. Genes Dev. **3:**1288–1300.
2. **Belsham, G. J., and J. K. Brangwyn.** 1990. A region of the 5′ noncoding region of foot-and-mouth disease virus RNA directs efficient internal initiation of protein synthesis within cells: involvement with the role of L protease in translation control. J. Virol. **64:**5389–5395.
3. **Bier, E., H. Vaessin, S. Sheperd, K. Lee, K. McCall, S. Barbel, L. Ackerman, R. Carretto, T. Uemura, E. Grell, L. Y. Jan, and Y. N. Jan.** 1989. Searching for pattern and mutation in the *Drosophila* genome with a *P-lacZ* vector. Genes Dev. **3:**1273–1287.
4. **Bonneau, A., and N. Sonenberg.** 1987. Involvement of the 24-kDa Cap-binding protein in regulation of protein synthesis in mitosis. J. Biol. Chem. **262:**11134–11139.
5. **Borman, A., M. T. Howell, J. G. Patton, and R. J. Jackson.** 1993. The involvement of a spliceosome component in internal initiation of human rhinovirus RNA translation. J. Gen. Virol. **74:**1775–1788.
6. **Burn, T. C., J. O. Vigoreaux, and S. L. Tobin.** 1989. Alternative 5C actin transcripts are localized in different patterns during Drosophila embryogenesis. Dev. Biol. **131:**345–355.
7. **Campos-Ortega, J. A., and V. Hartenstein.** 1985. The embryonic development of Drosophila melanogaster. Springer-Verlag, New York, N.Y.
8. **Carroll, S. B., S. DiNardo, P. H. O'Farrel, R. A. H. White, and M. P. Scott.** 1988. Temporal and spatial relationships between segmentation and homeotic gene expression in *Drosophila* embryos: distribution of the fushi tarazu, engrailed, sex combs reduced, Antennapedia and Ultrabithorax proteins. Genes Dev. **2:**350–360.
9. **Cavener, D., G. Corbett, D. Cox, and R. Whetten.** 1986. Isolation of the eclosion gene cluster and the developmental expression of the *Gld* gene in *Drosophila melanogaster*. EMBO J. **5:**2939–2948.
10. **Cavener, D. R., and B. A. Cavener.** 1993. Translation start sites and mRNA leaders, p. 359–377. *In* G. Maroni (ed.), An atlas of Drosophila genes. Oxford University Press, Oxford, United Kingdom.
11. **Cavener, D. R., and S. C. Ray.** 1991. Eukaryotic start and stop translation sites. Nucleic Acids Res. **19:**3185–3192.
12. **Feng, Y., L. E. Gunter, E. L. Organ, and D. R. Cavener.** 1991. Translation initiation in *Drosophila melanogaster* is reduced by mutations upstream of the AUG initiator codon. Mol. Cell. Biol. **11:**2149–2153.
13. **Glaser, R. L., M. F. Wolfner, and J. T. Lis.** 1986. Spatial and temporal pattern of *hsp26* expression during normal development. EMBO J. **5:**747–754.
14. **Haller, A. A., and B. L. Semler.** 1992. Linker scanning mutagenesis of the internal ribosome entry site of poliovirus RNA. J. Virol. **66:**5075–5086.
15. **Huang, J., and R. J. Schneider.** 1991. Adenovirus inhibition of cellular protein synthesis involves inactivation of cap-binding protein. Cell **65:**271–280.
16. **Jang, S. K., M. V. Davies, R. J. Kaufman, and E. Wimmer.** 1989. Initiation of protein synthesis by internal entry of ribosomes into the 5′ nontranslated region of encephalomyocarditis virus RNA in vivo. J. Virol. **63:**1651–1660.
17. **Jang, S. K., and E. Wimmer.** 1990. Cap-independent translation of encephalomyocarditis virus RNA: structural elements of the internal ribosomal entry site and involvement of a cellular 57-kD RNA-binding protein. Genes Dev. **4:**1560–1572.
18. **Kaminski, A., M. T. Howell, and R. J. Jackson.** 1990. Initiation of encephalomyocarditis virus RNA translation: the authentic initiation site is not selected by a scanning mechanism. EMBO J. **9:**3753–3759.
19. **Kim, D. G., H. M. Kang, S. K. Jang, and H.-S. Shin.** 1992. Construction of a bifunctional mRNA in the mouse by using the internal ribosomal entry site of the encephalomyocarditis virus. Mol. Cell. Biol. **12:**3636–3643.
20. **Knipple, D. C., and R. J. MacIntyre.** 1984. Cytogenetic mapping and isolation of mutations of the β-Gal-1 locus of *Drosophila melanogaster*. Mol. Gen. Genet. **198:**75–83.
21. **Kozak, M.** 1989. The scanning model for translation: an update. J. Cell Biol. **108:**229–241.
22. **Kozak, M.** 1991. An analysis of vertebrate mRNA sequences: intimations of translational control. J. Cell. Biol. **115:**887–903.
23. **Lin, T. A., X. Kong, T. A. Haystead, A. Pause, G. Belsham, N. Sonenberg, and J. C. Lawrence, Jr.** 1994. PHAS-I as a link between mitogen-activated protein kinase and translation initiation. Science **266:**653–656.
24. **Macejak, D. G., and P. Sarnow.** 1991. Internal initiation of translation mediated by the 5′ leader of a cellular mRNA. Nature **353:**90–94.
25. **Meerovitch, K., J. Pelletier, and N. Sonenberg.** 1989. A cellular protein that binds to the 5′-noncoding region of poliovirus RNA: implications for internal translation initiation. Genes Dev. **3:**1026–1034.
26. **Mueller, P., and A. Hinnebusch.** 1986. Multiple upstream AUG codons mediate translational control of GCN4. Cell **45:**201–207.
27. **Neumann, J. R., C. A. Morency, and K. O. Russian.** 1987. A novel rapid assay for chloramphenicol acetyltransferase gene expression. BioTechniques **5:**444–447.
28. **OH, S. K., M. P. Scott, and P. Sarnow.** 1992. Homeotic gene Antennapedia mRNA contains 5′-noncoding sequences that confer translational initiation by internal ribosome binding. Genes Dev. **6:**1643–1653.
29. **Pause, A., G. J. Belsham, A.-C. Gingras, O. Donze, T.-A. Lin, J. C. Lawrence, Jr., and N. Sonenberg.** 1994. Insulin-dependent stimulation of protein synthesis by phosphorylation of a regulator of 5′-cap function. Nature **371:**762–767.
30. **Pelletier, J., and N. Sonenberg.** 1988. Internal initiation of translation of eukaryotic mRNA directed by a sequence derived from poliovirus RNA. Nature **334:**320–325.
31. **Robertson, H. M., C. R. Preston, R. W. Phillis, D. M. Johnson-Schlitz, W. K. Benz, and W. R. Engels.** 1988. A stable source of P-element transposase in *Drosophila melanogaster*. Genetics **118:**461–470.
32. **Rubin, G. M., and A. C. Spradling.** 1983. Genetic transformation of *Drosophila* with transposable element vectors. Science **218:**348–353.
33. **Sarnow, P.** 1989. Translation of glucose-regulated protein 78/immunoglobulin heavy-chain binding protein mRNA is increased in poliovirus-infected cells at a time when cap-dependent translation of cellular mRNAs is inhibited. Proc. Natl. Acad. Sci. USA **86:**5795–5799.
34. **Simon, J. A., and J. T. Lis.** 1987. A germline transformation analysis reveals flexibility in the organization of the heat shock consensus elements. Nucleic Acids Res. **15:**2971–2988.
35. **Sonenberg, N., and K. Meerovitch.** 1990. Translation of poliovirus mRNA. Enzyme **44:**278–291.
36. **Svitkin, Y. V., K. Meerovitch, and N. Sonenberg.** 1994. Internal translation initiation on poliovirus RNA: further characterization of La function in poliovirus translation in vitro. J. Virol. **68:**1544–1550.
37. **Tautz, D., and C. Pfeifle.** 1989. A non-radioactive *in situ* hybridization method for the localization of specific RNAs in Drosophila embryos reveals translational control of the segmentation gene hunchback. Chromosoma **98:**81–85.
38. **Thummel, C. S., A. M. Boulet, and H. D. Lipshitz.** 1990. Vectors for *Drosophila* P element mediated transformation and tissue culture transfection. Gene **74:**445–456.

38a. **Tolias, P.** Personal communication.

39. **Vagner, S., M. C. Gensac, A. Maret, F. Bayard, F. Amalric, H. Prats, and A. C. Prats.** 1995. Alternative translation of human fibroblast growth factor 2 mRNA occurs by internal entry of ribosomes. Mol. Cell. Biol. **15:**35–44.
40. **White, R. A. H., and M. Wilcox.** 1985. Distribution of Ultrabithorax proteins in Drosophila. EMBO J. **4:**2035–2043.